

# Rod-like defects in silicon: signatures of distinct RLD structures detected by various measurement methods

T. Mchedlidze

*IHP/BTU JointLab, BTU Cottbus*

# Starting remarks

---

## History

1991~1992 and 2002~2003, IMR Sendai

From 2005, JointLab, Cottbus

## Publications

- T. Mchedlidze, V. V. Kveder, J. Jablonski, and K. Sumino, Phys. Rev. B **50**, 1511 (1994).
- T. Mchedlidze and M. Suezawa, Phys. Rev. B **70**, 205203 (2004).
- T. Mchedlidze, S. Binetti, A. Le Donne, S. Pizzini and M. Suezawa, J. Appl. Phys. **98**, 043507 (2005).
- T. Mchedlidze, S. Binetti, A. Le Donne, S. Pizzini and M. Suezawa, Phys. Stat. Sol. (c) **2**, 1807 (2005).

## Acknowledgements

Cordial thanks are due to:

Vitaly V. Kveder

Koji Sumino

Masashi Suezawa

# Outline

---

## ❖ Reviewing what was known

- ❖ Interstitial agglomerates in Si
- ❖ Transmission electron microscopy
- ❖ Theoretical calculations
- ❖ Photoluminescence and deep level transient spectroscopy
- ❖ Electric-dipole spin resonance

## ❖ Experimental

- ❖ Samples, measurement technique

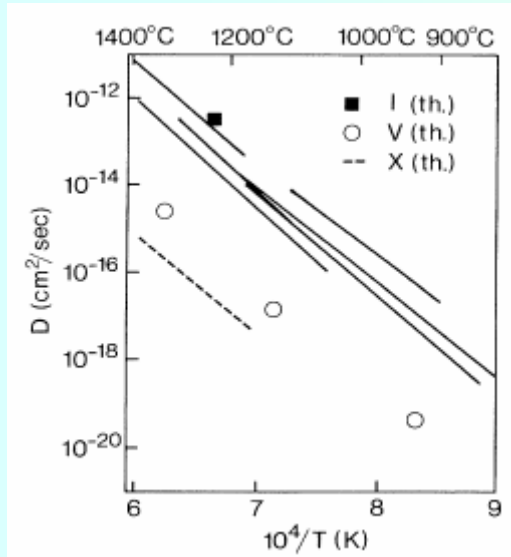
## ❖ Signatures of rod-like defects

- ❖ Deep level transient spectroscopy
- ❖ Photoluminescence

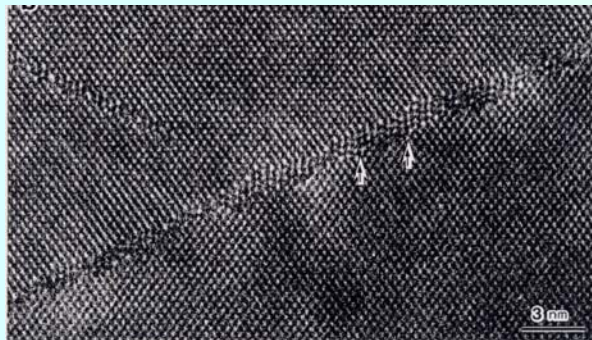
## ❖ Summary

# Self-interstitials in Si

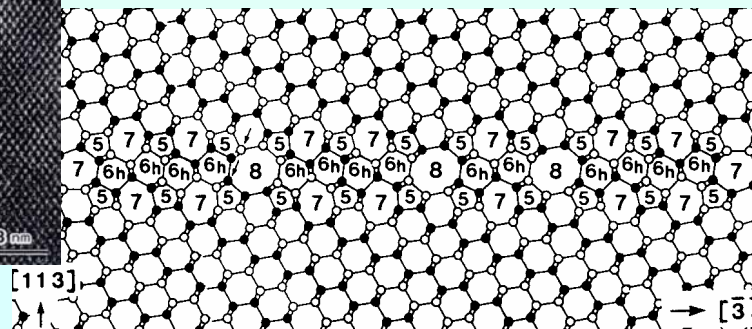
## Diffusion processes (TED)



P.E. Blochl et al., PRL **70**(1993)2435

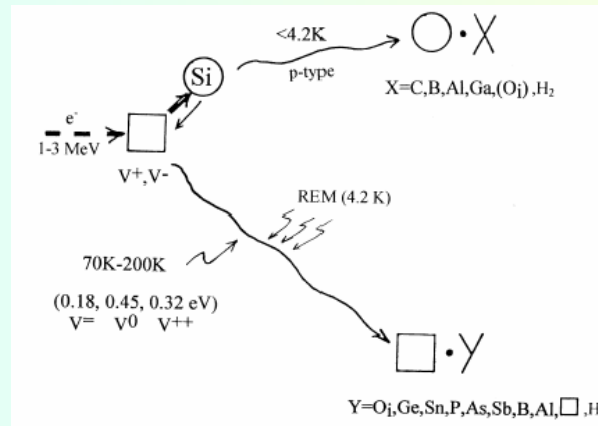


## {311} structural defects



S.Takeda et.al., Phil.Mag.**70**(1994)287

## Defect reactions

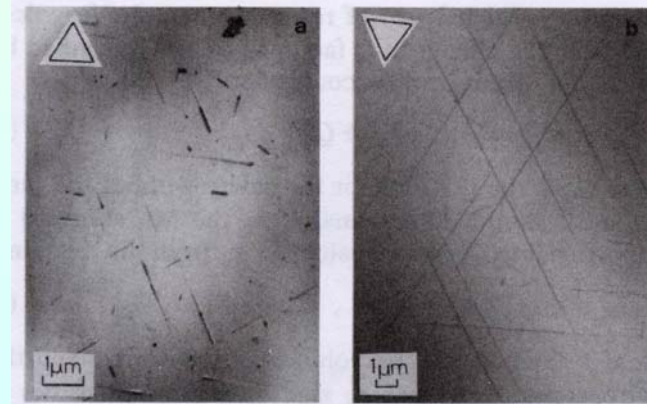


G.D. Watkins, Mat. Sci. in Semicond. Processing **3**(2000)227

## Thermal donors in silicon: oxygen clusters or self-interstitial aggregates?

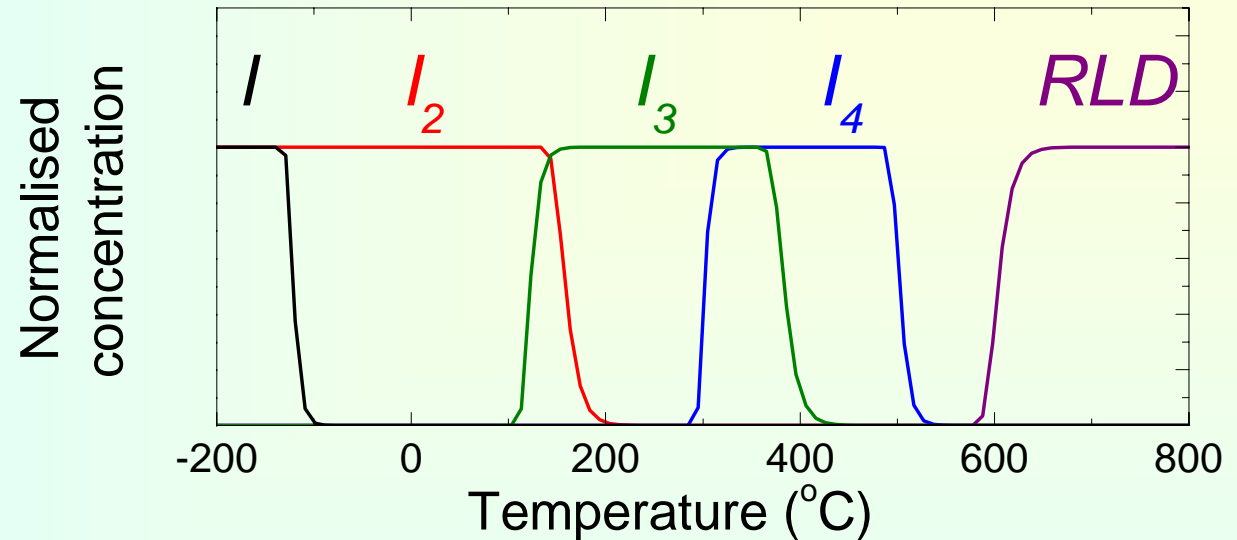
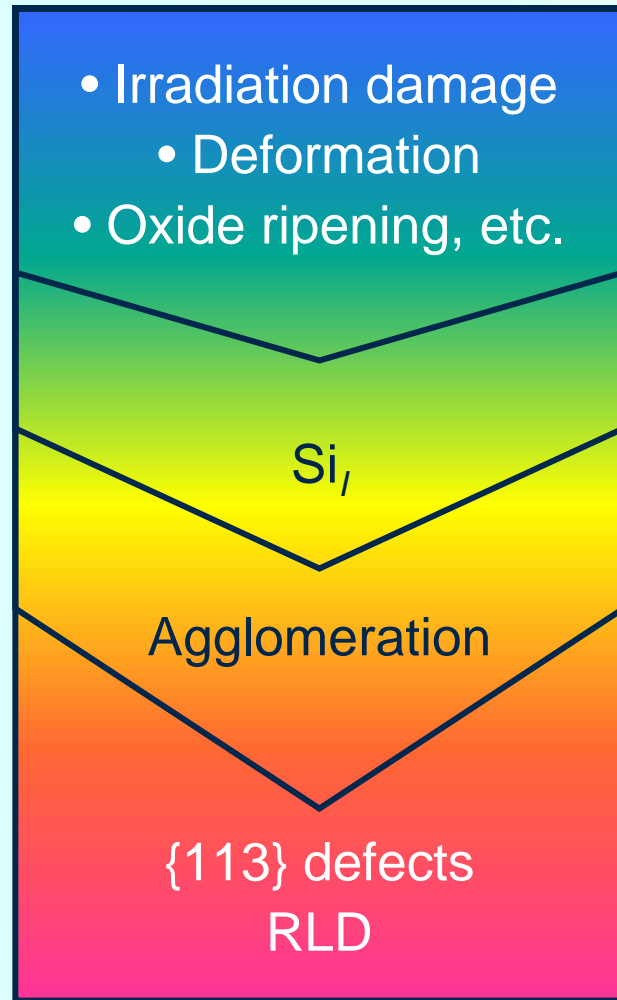
R.C. Newman, J.Phys.C: Sol.St.Phys.**18**(1985)L967

## Rod-like defects



T.Mchedlidze et al., PRB **50**(1994)1511

# Formation of self-interstitial agglomerates



? Properties of small clusters

? Formation mechanism:

? ripening ( $I_n + I \rightarrow I_{n+1}$ ) or

? special role of  $I_4$  and  $I_8$  ( $I_n + I_k \rightarrow I_{n+k}$ )

? Role of impurities (H, O, C, Fe...)

# *Properties of self-interstitial agglomerates*

---

## Theoretical calculations:

- B. J. Coomer, et. al., J.Phys.: Condens. Matter **13**, L1 (2001).
- P. Alippi and L. Colombo, Phys. Rev. B **62**, 1815 (2000).
- J. Kim, et. al., Phys. Rev. Lett., **84**, 503 (2000).
- J. P. Goss, et. al., Appl. Phys. Lett., **85**, 4633 (2004).

## Transmission electron microscopy:

- S. Takeda, Jpn. J. Appl. Phys. **30**, L639 (1991);
- M. Kohyama and S. Takeda, Phys. Rev. B **46**, 12 305 (1992).

## Electrical and optical investigations:

- J. L Benton, S. Libertino, S. Coffa, et. al., Appl. Phys. Lett., 71, 389 (1997); J. Appl. Phys., 82, 120 (1997); J. Appl. Phys., 84, 4749 (1998); Phys. Rev. B, 63, 195206 (2001).
- P. K Giri, Semicond. Sci. and Technol., **20**, 638 (2005).

## Spin resonance investigations:

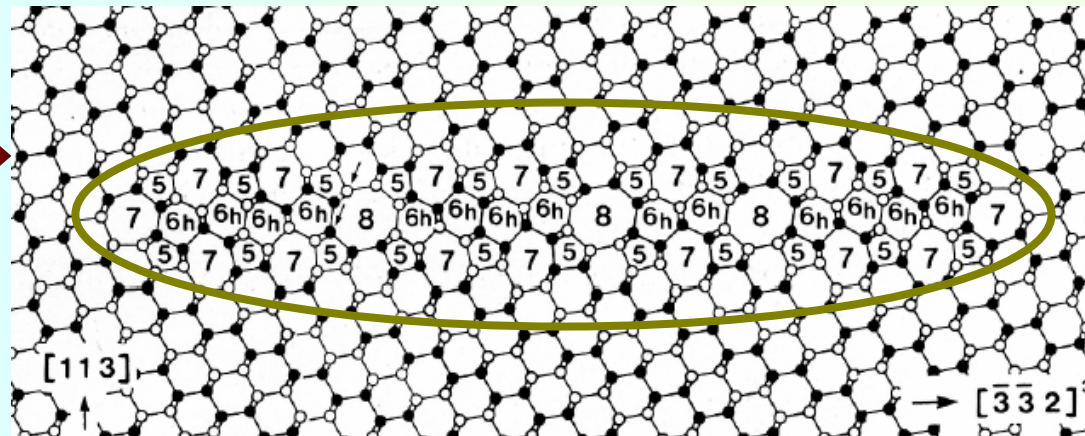
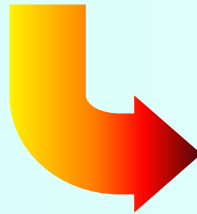
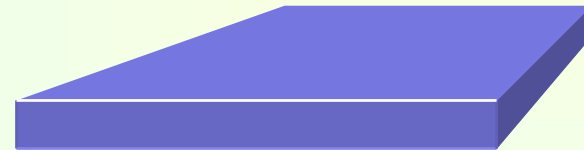
- T. Mchedlidze, et. al., Phys. Rev. B **50**, 1511 (1994).
- D. Pierreux and A. Stesmans, Phys. Rev. B **68**, 193208 (2003).
- T. Mchedlidze and M. Suezawa, Phys. Rev. B, **70**, 205203 (2004).
- T. Mchedlidze, et. al., J. Appl. Phys. **98**, 043507 (2005).



A micrograph showing a polymer blend with two large, bright, circular domains (likely crystalline regions) surrounded by a darker matrix. The domains are outlined with green dashed lines.



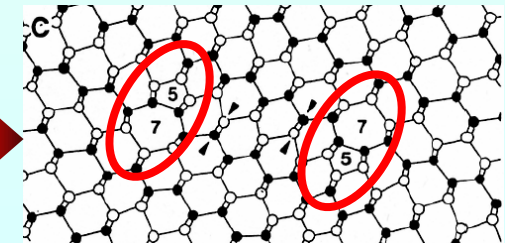
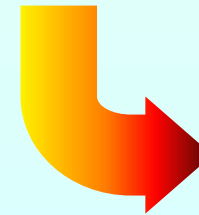
PD



DD

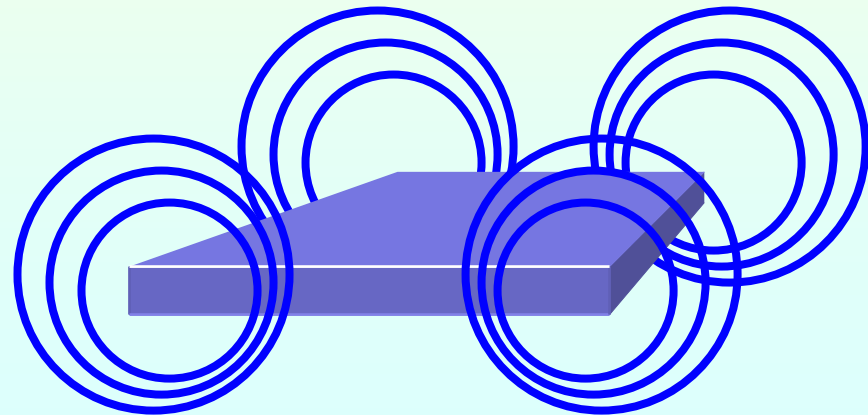
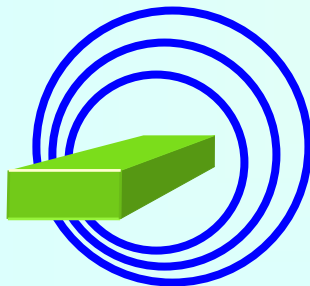
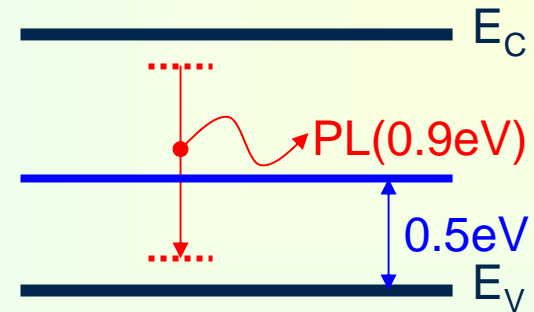
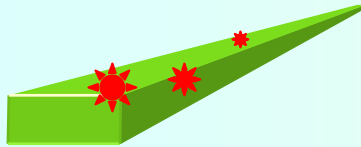


~~⊗~~  $[1\bar{1}0]$



© 2006 - All rights reserved

# *RLD – {113} structural defects - theory*



J. P. Goss, et. al., Appl. Phys. Lett., **85**, 4633 (2004).



# RLD – {113} structural defects – DLTS, PL

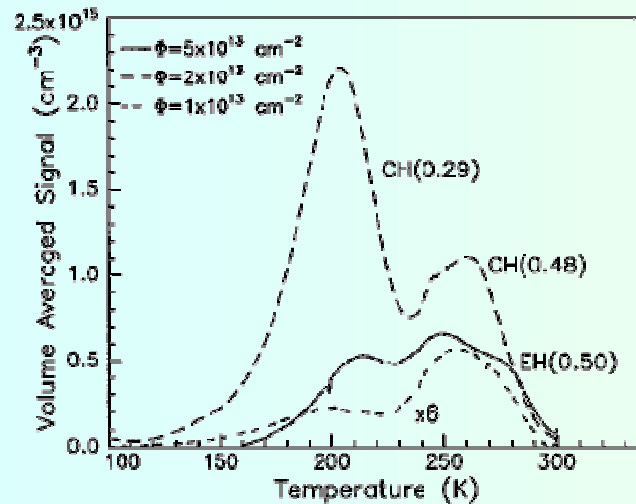


FIG. 5. DLTS spectra after 145 keV Si ion implantation and thermal anneal of 685 °C, 1 h. The concentration of cluster defects increases as the dose is raised from  $1 \times 10^{13}$  to  $2 \times 10^{13}$  Si/cm<sup>2</sup>. At a fluence of  $5 \times 10^{13}$  Si/cm<sup>2</sup>, the total concentration of cluster defects is dramatically reduced and the extended defect signature, EH(0.50 eV), is observed.

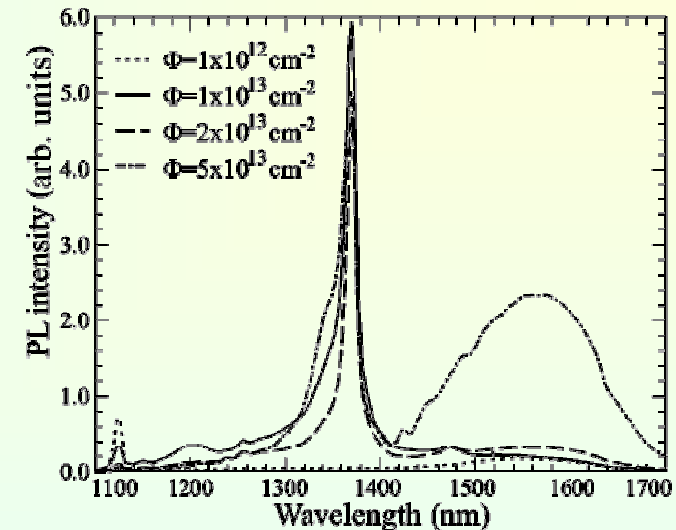
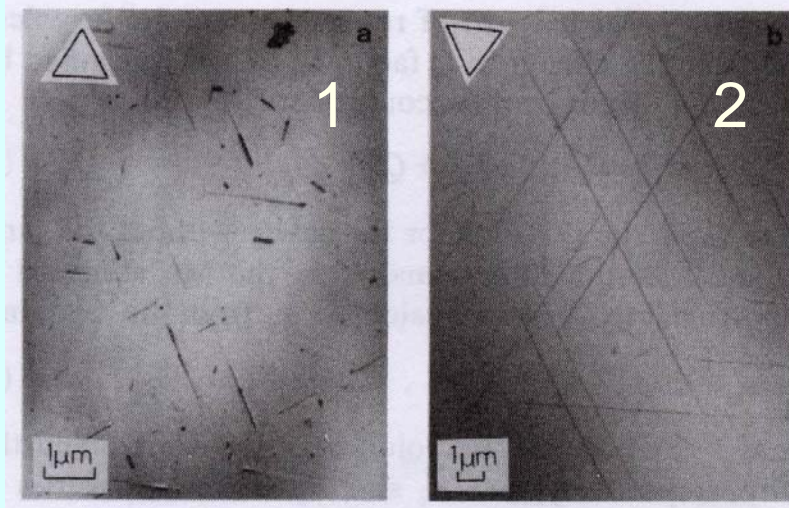


FIG. 18. PL spectra taken at 17 K on *n*-type Si samples implanted with 1.2 MeV Si to doses of  $1 \times 10^{12} \text{ cm}^{-2}$  (dotted line),  $1 \times 10^{13} \text{ cm}^{-2}$  (solid line),  $2 \times 10^{13} \text{ cm}^{-2}$  (dashed line), and  $5 \times 10^{13} \text{ cm}^{-2}$  (dash-dot-dashed line). The samples have been annealed at 680 °C for 1 h.

- High-dose implantation,  $>10^{13}$  Si/cm<sup>2</sup>, and annealing at temperatures above 680°C causes the {311} extended defect formation.
- The {311} defect presence is detectable by both electrical (with a signature at  $E_V+0.5$  eV) and optical (with a PL signal at 1376 nm) measurements.

J. L Benton, S. Libertino, S. Coffa, et. al.

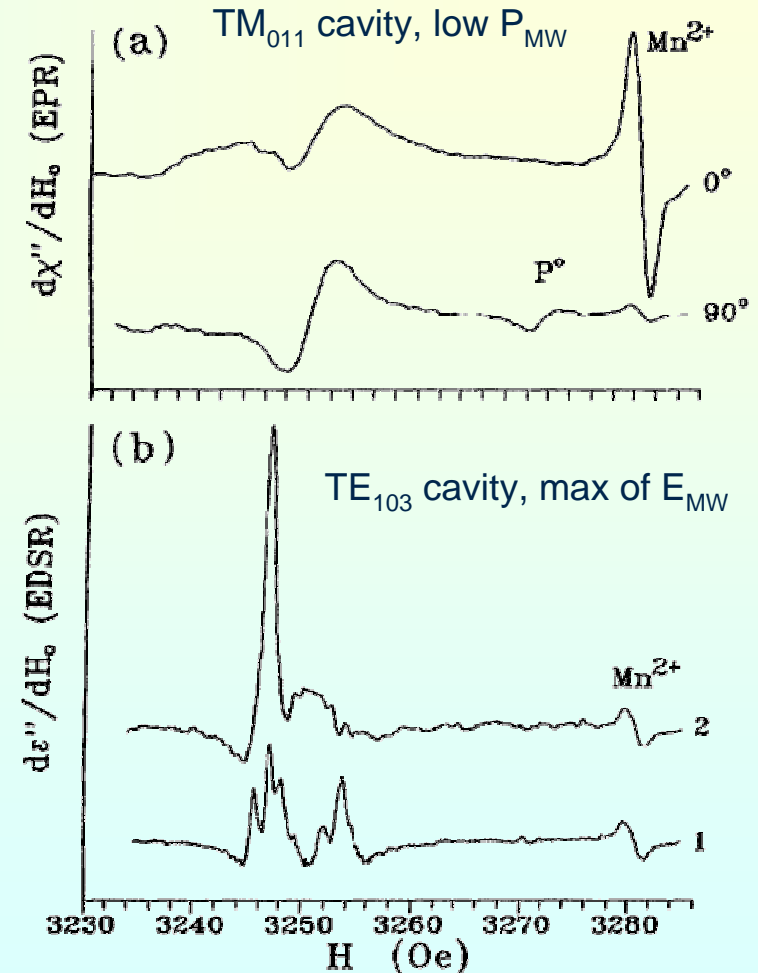
# RLD – {113} structural defects – EDSR



From dependencies of intensity and shape of the EDSR signals on temperature and MW power it was determined that:

- Relatively deep quasi-one-dimensional energy band is associated with RLDs
- Localization length of electrons along RLDs is of 100 nm order.
- Electron mobility in the band at 10K is more than 500 cm<sup>2</sup>/V.

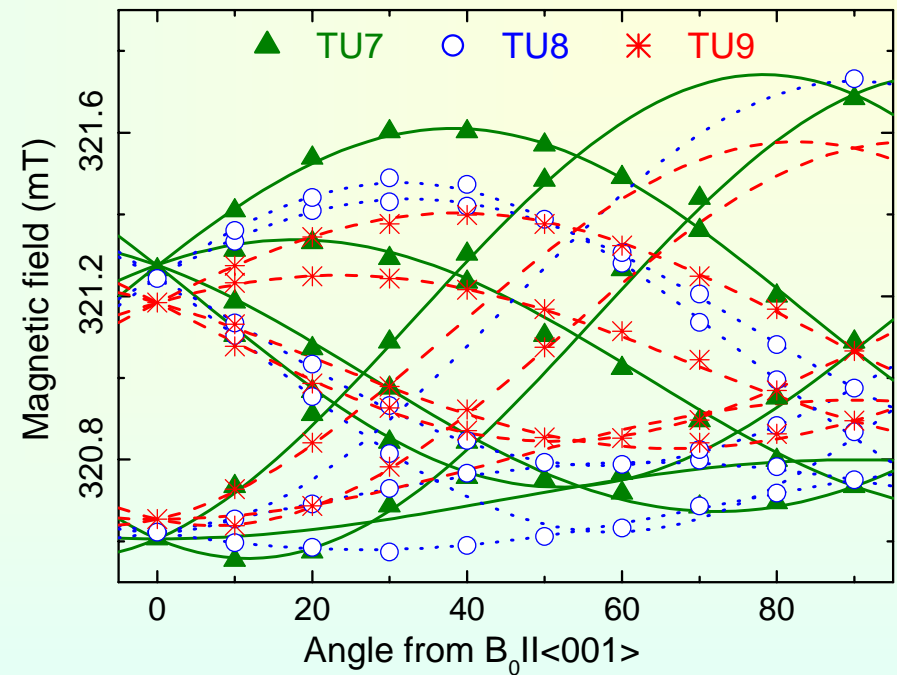
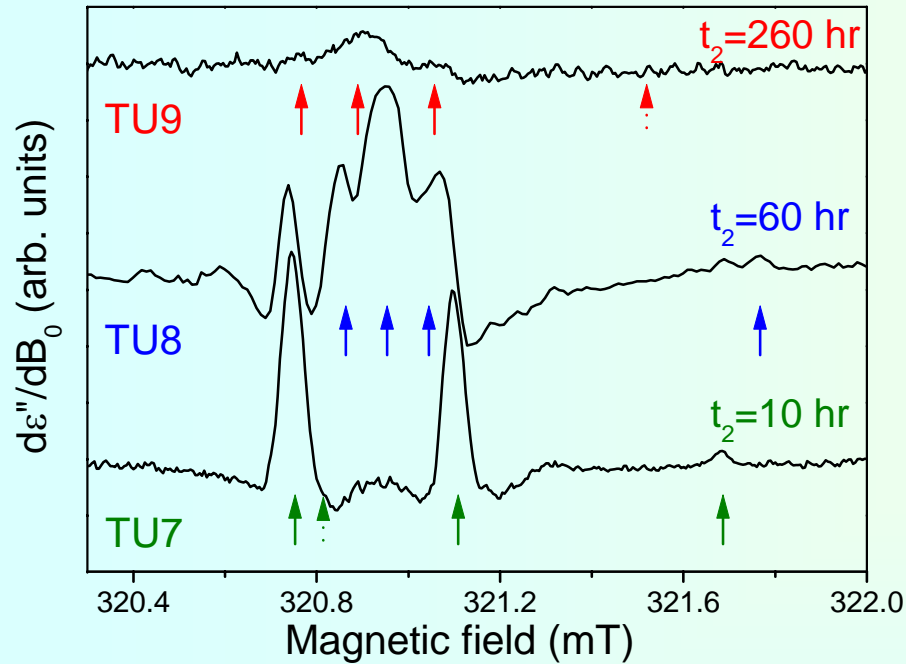
T. Mchedlidze, et. al., Phys. Rev. B **50**, 1511 (1994).



# Samples

- ❖ Phosphorus-doped Cz-Si crystals.
- ❖ Initial resistivity of  $0.8 \Omega\text{cm}$ .
- ❖ Interstitial oxygen concentration of  $25 \times 10^{17} \text{ cm}^{-3}$ .
- ❖ Pre-annealing in evacuated quartz capsules at  $450^\circ\text{C}$  for 160 h.
- ❖ Subsequent annealing at  $650^\circ\text{C}$  for
  - ❖ 10 h (sample “S”)
  - ❖ 60 h (sample “M”)
  - ❖ 260 h (sample “L”)

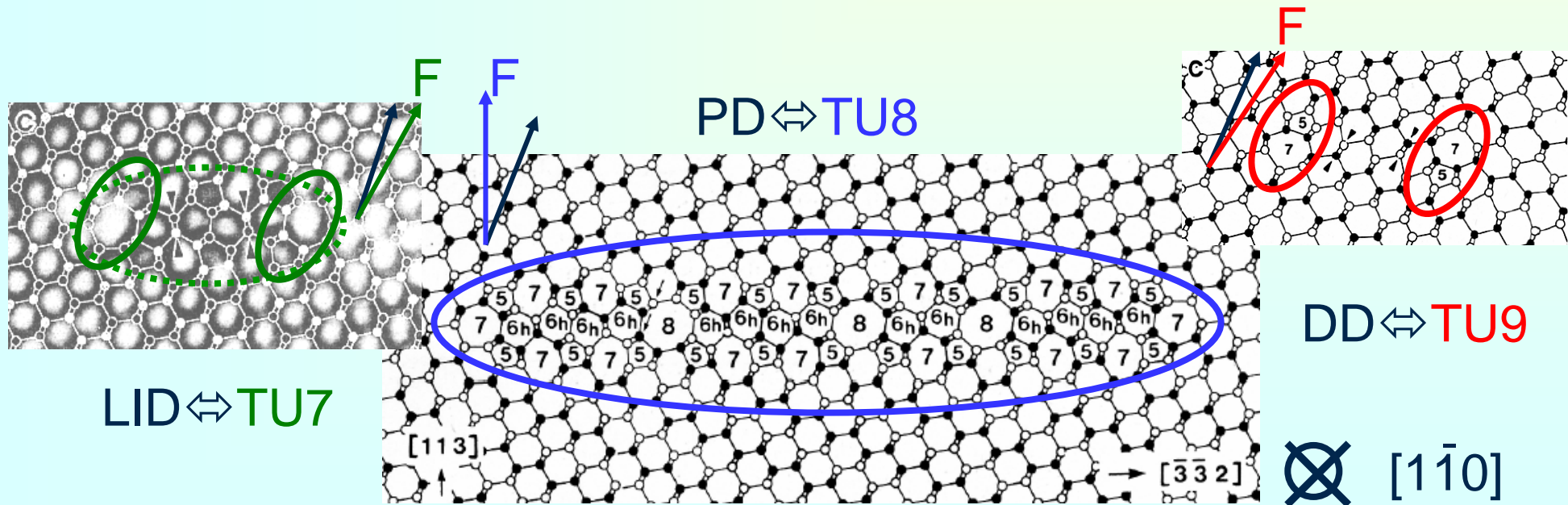
# Identification of EDSR signals from RLDs



Center	Spin	System	$g_1$	$g_2$	$g_3$	$\theta$	Defect
TU7	$\frac{1}{2}$	$C_{1V}$	2.0005	1.9946	2.0020	12	LID
TU8			1.9947	2.0005	2.0018	27	PD
TU9			1.9996	1.9957	2.0015	9	DD

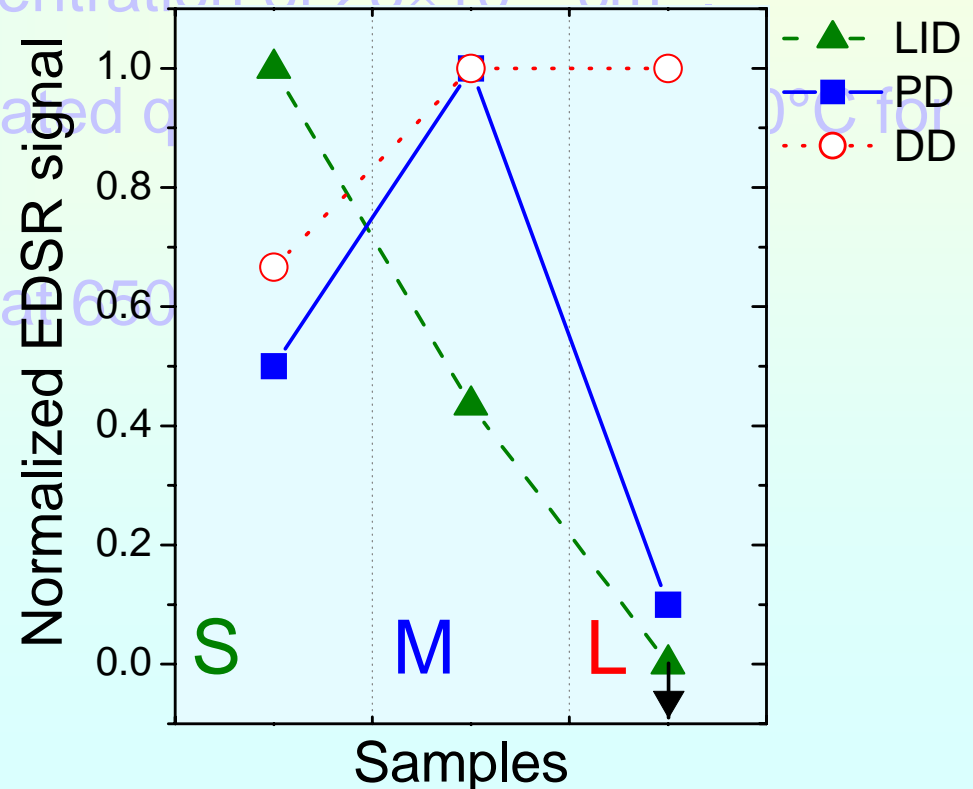
# Identification of EDSR signals from RLDs

- Symmetry of the TU7-TU9 centers fits that expected for the RLD structures. Moreover, the directions for the main axes of g tensors closely fits those expected for the RLD structures, i.e.,  $\sim[113]$  for PDs and  $\sim[115]$  for LIDs and DDs.
- Formation kinetics for the EDSR signals and related RLD structures also well correlates.



# Samples pre-characterized by EDSR

- ❖ Phosphorus-doped Cz-Si crystals.
- ❖ Initial resistivity of  $0.8 \Omega\text{cm}$ .
- ❖ Interstitial oxygen concentration of  $25 \times 10^{17} \text{ cm}^{-3}$
- ❖ Pre-annealing in evacuated quartz tube at  $650^\circ\text{C}$  for 160 h.
- ❖ Subsequent annealing at  $650^\circ\text{C}$  for
  - ❖ 10 h (sample "S")
  - ❖ 60 h (sample "M")
  - ❖ 260 h (sample "L")



# Experimental

## *DLTS measurements:*

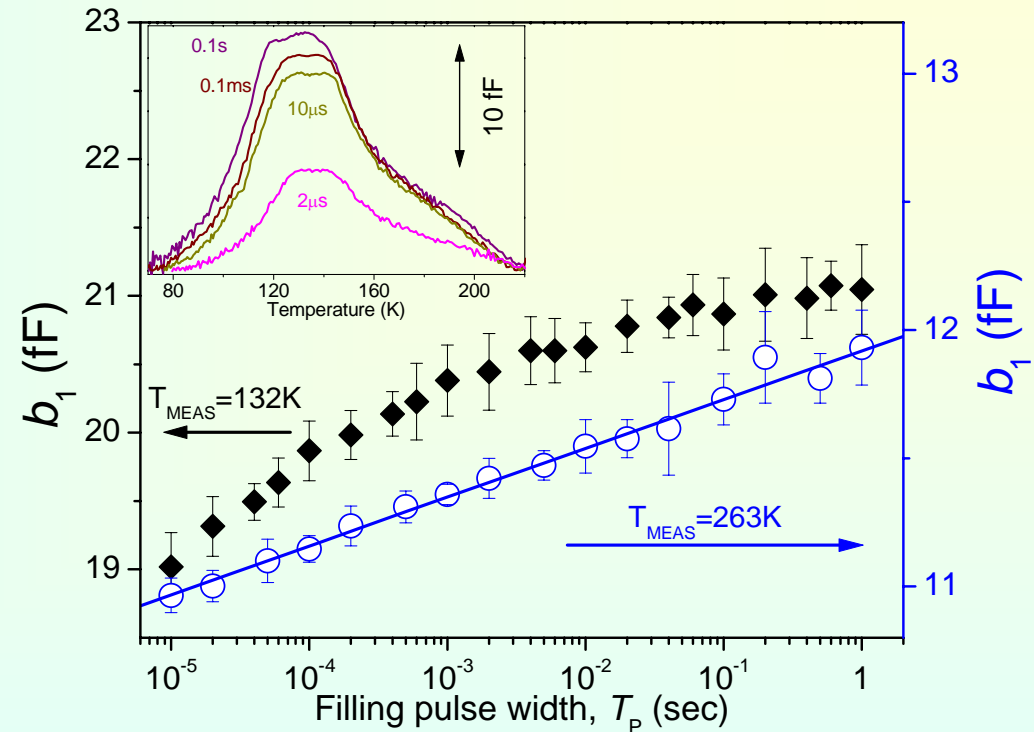
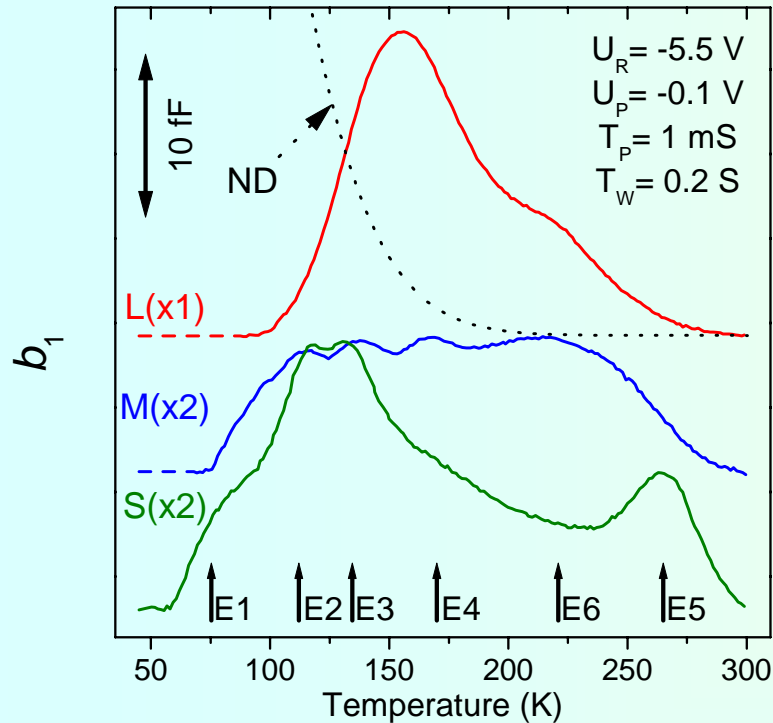
- Au Schottky contacts,  $\varnothing$  0.7 mm.
- Ohmic contacts: GaIn alloy.
- Transient Fourier spectroscopy DL-8000 system (Accent).  $T_{\text{MEAS}}$ : 20 ÷ 300 K.
- Representative DLTS spectra change of  $b_1$  Furrier coefficient with temperature ( $T_{\text{MEAS}}$ ) and/or with sampling period ( $T_{\text{W}}$ ).

## *PL measurements:*

- Excitation with Ar-ion laser:
  - $\lambda = 454$  nm
  - Power density: 10 ÷ 1000 W/cm<sup>2</sup>
- $T_{\text{MEAS}}$ : 5 ÷ 300 K.
- PL system: monochromator → N<sub>2</sub> cooled Ge-detector + laser-beam chopper and a lock-in system.
- Detection range 0.7-1.5 eV.



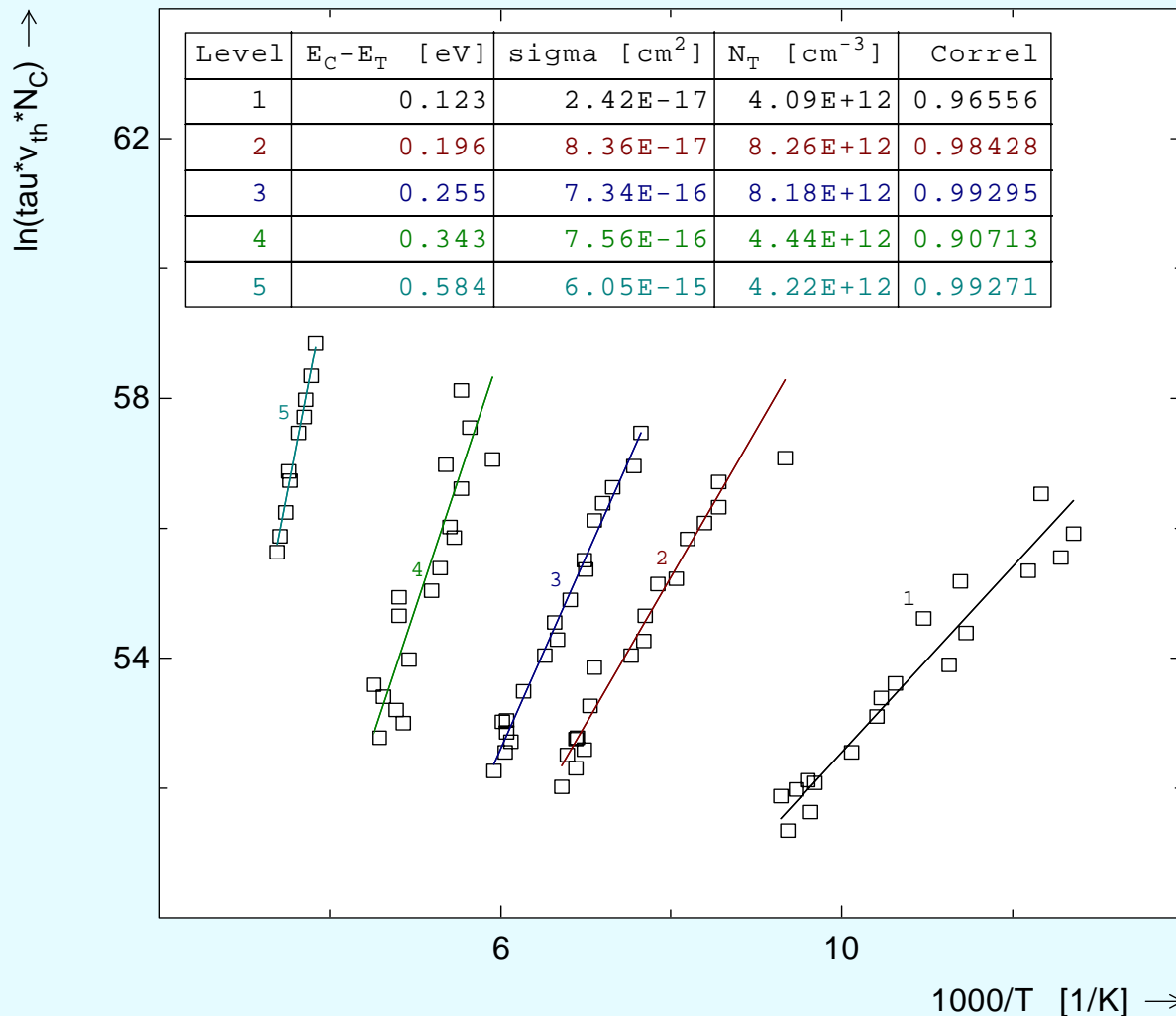
# Results: DLTS



## Character of defect states:

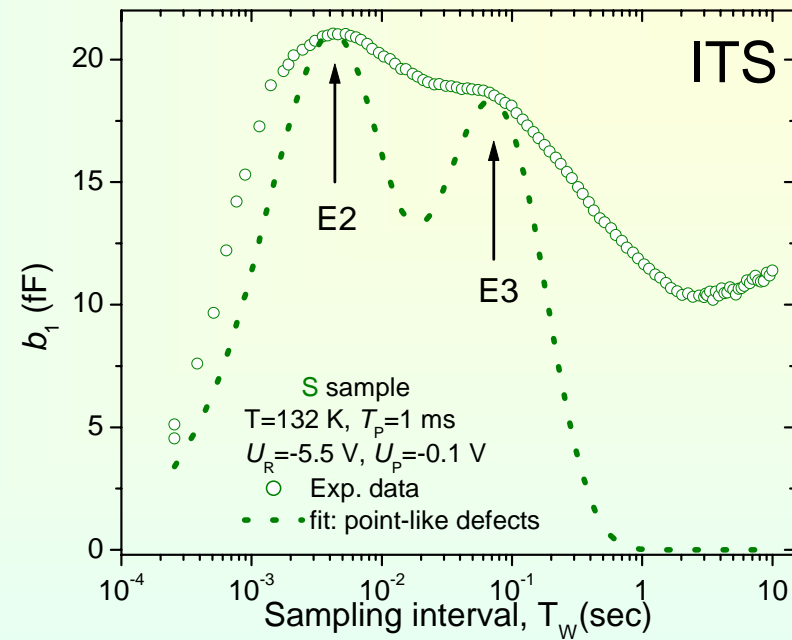
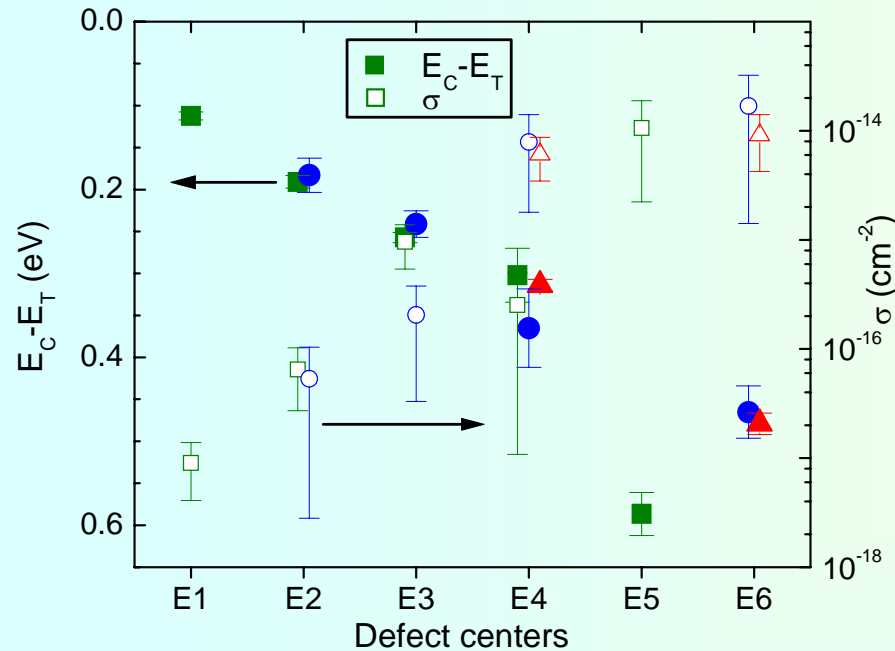
- $E_2$  &  $E_3$  are extended defects with band-like states;
- $E_5$  are extended defects with localized states.  $E_4$  &  $E_6$  are extended defects;
- $E_1$  character of defects states couldn't be determined.

# Results: DLTS: Arrhenius plot (example)



Name = @A\_001.ATA  
 Comm = Rodlikes in ch5  
 new soft  
 ID = CH5  
 rcID = 0000  
 Date = 08/15/2006  
 Type = n-Si  
 Area = 3.95E-03 cm<sup>2</sup>  
 $N_S$  = 4.32E+14 cm<sup>-3</sup>  
 $T_W$  = 2.05 ms  
 $t_P$  = 1.00 ms  
 $U_R$  = -5.50 V  
 $U_P$  = -0.10 V

# Results: DLTS



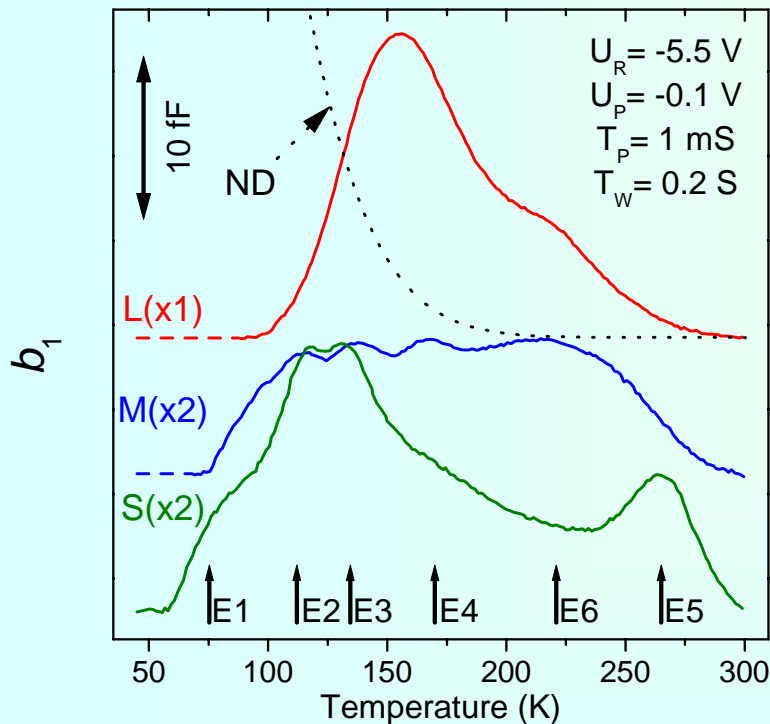
- Scatter of  $E_C - E_T$  and  $\sigma$  parameters is related to extended character of states.
- Estimations of trap density is not valid;  $E_C - E_T$  and  $\sigma$  are only rough estimates.
- From Isothermal Transient Spectrum detected at 132K and from fitting of this spectrum with point-like defect model:  $N(E_2) = N(E_3)$ .

## Attribution by change in signal intensity:

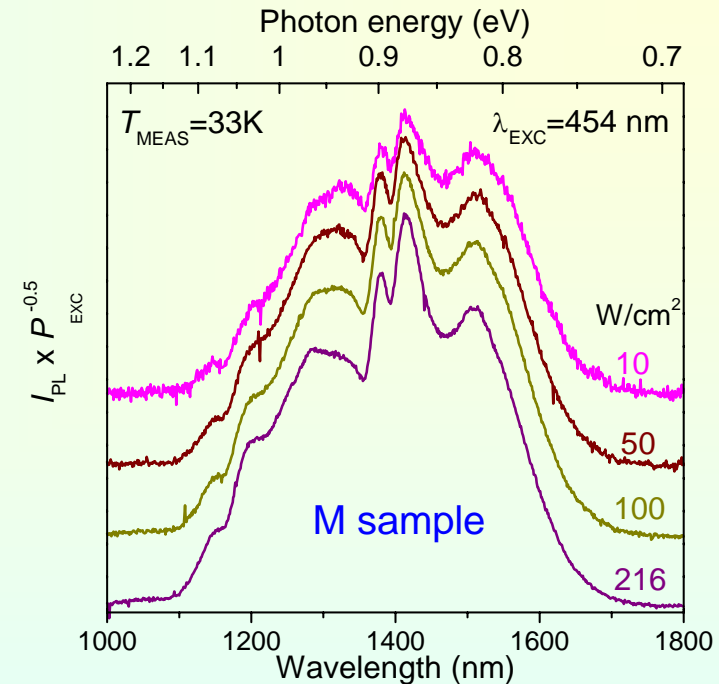
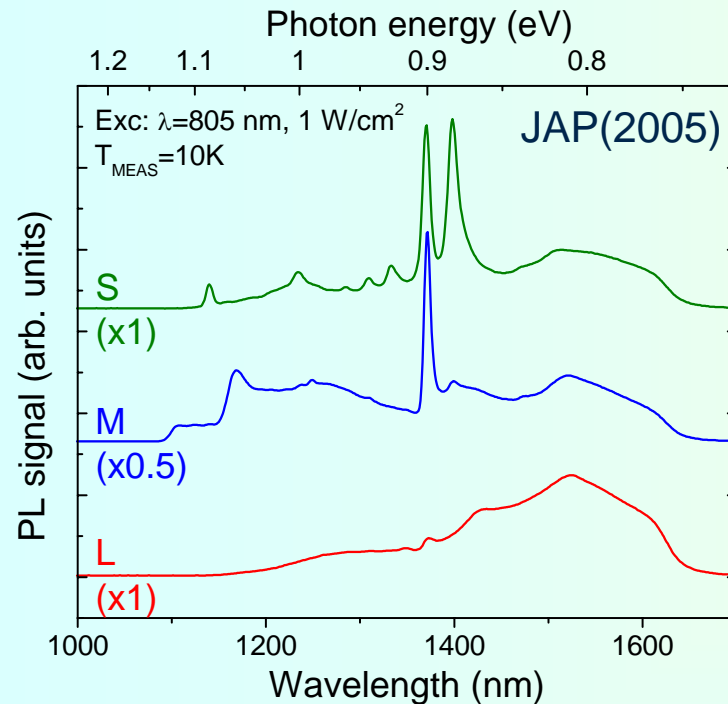
- $E_2(\sim 0.2 \text{ eV})$  &  $E_3(\sim 0.25 \text{ eV})$  – LID
- $E_5(\sim 0.59 \text{ eV})$  – LID (?)
- $E_4(\sim 0.35 \text{ eV})$  – DD
- $E_6(\sim 0.48 \text{ eV})$  – PD
- $E_1(\sim 0.11 \text{ eV})$  – ??

## Attribution by character of states:

- $E_2, E_3$  – LID, localized along defects
- $E_5$  – LID, defects in structure or non-RLD
- $E_4$  – DD, localized and band-like states
- $E_6$  – PD, localized and band-like states
- $E_1$  – non-RLD (?)

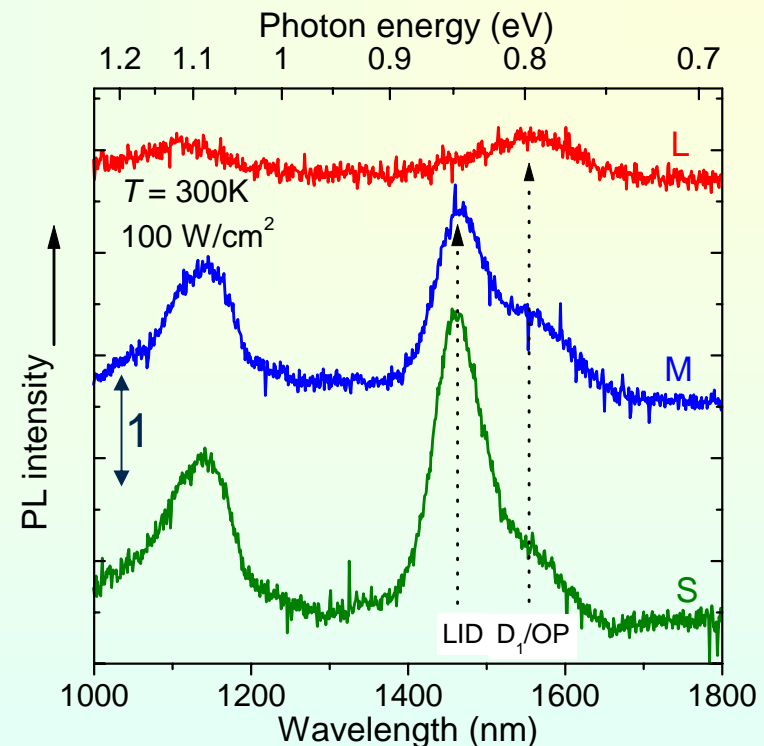
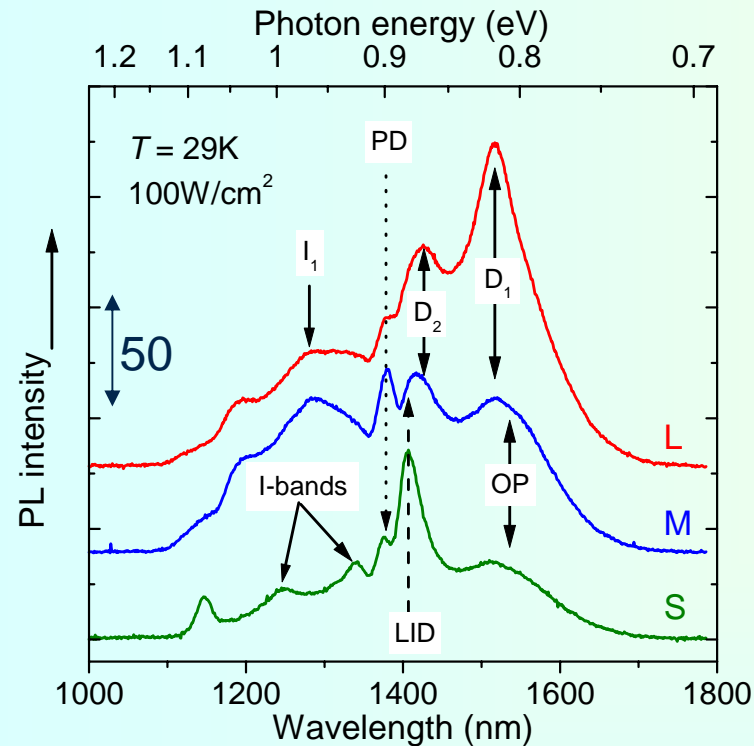


# Results: PL



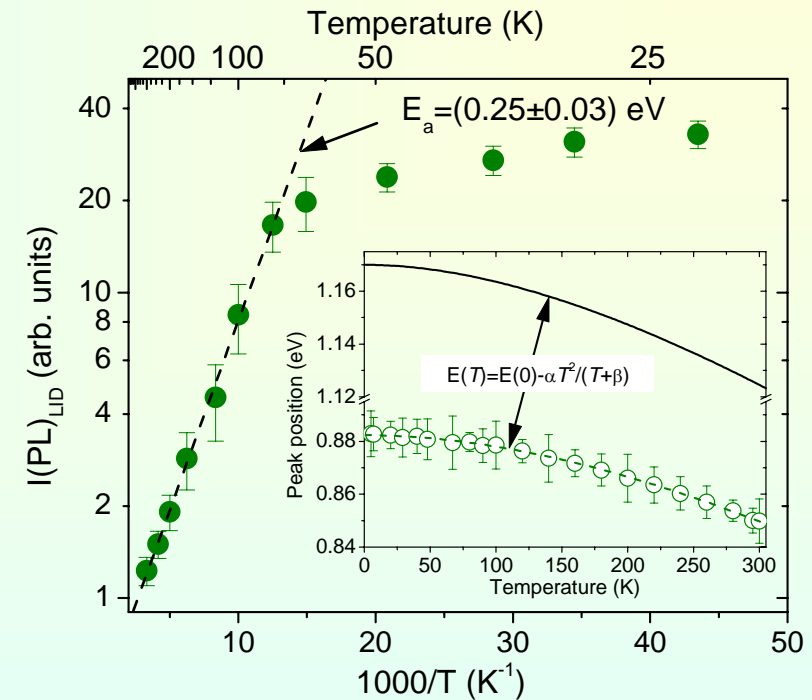
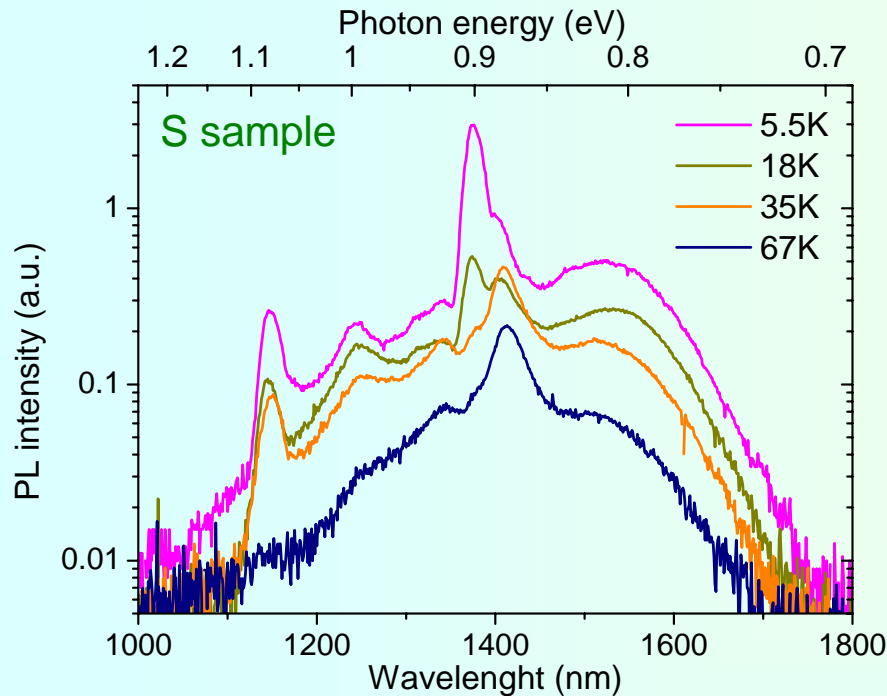
- Small power density was used previously to achieve maximal resolution.
- To excite possibly large number of transitions and suppress influence of variation in recombination cross-sections, possibly high power density should be used for excitation.
- Excess power density may cause loss of resolution and local heating.

# Results: PL



- For all  $T_{\text{MEAS}}$  the PL spectra for S, M and L samples differed significantly.
- Assignment of PL peaks was done according to EDSR results for samples and using published data for PL peaks.
- Temperature behavior of peaks was complex.

# Results: PL



- Quenching of the LID peak intensity was observed from  $T_{\text{MEAS}} \geq 70$  K. Activation energy of this process,  $E_a \approx E_C - E_{\text{LID}}(\text{PL}) \approx 0.25 \text{ eV}$

$E(T) = E(0) - \alpha T^2 / (T + \beta)$	$E_T(0)$ (eV)	$\alpha$ ( $10^{-3} \text{ eV/K}$ )	$\beta$ (K)
Si band gap	1.17	4.7	636
LID	0.88	4.7	999



# Summary

## Line-interstitial defects:

- Appear at early stages of RLD formation
- They have extended band-like states

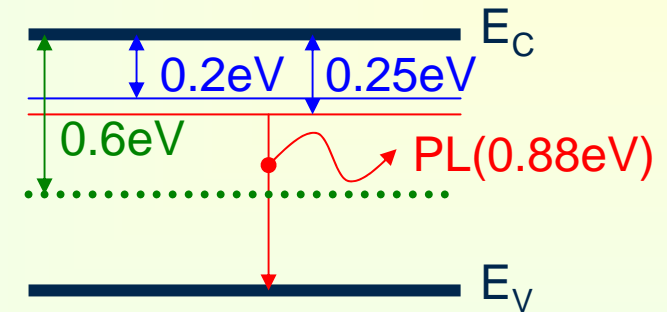
## Optical signatures:

**PL:** PL peak at 1405nm (0.88eV) at He temperatures. Peak persists up to room temperature, energy of the PL peak is shifted to ~1458nm (0.85eV). This peak corresponds to band-edge transition and could be observed even at room temperature.

## Electrical signatures:

**DLTS:** Pair of energy bands with similar density of states are positioned at ~0.2eV and ~0.25eV from the conduction band.

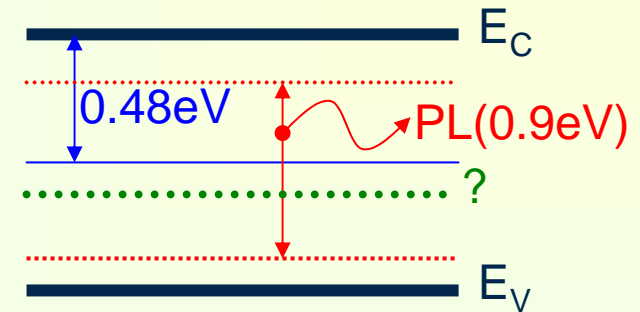
*Possibly* LID has also **deep extended localized states** located at ~0.6eV from conduction band. This states may be related to irregular parts of LIDs.



# Summary

## Plane defects:

- Appear at intermediate stages of RLD formation
- They have extended band-like states



## Optical signatures:

**PL:** Strong PL peak at 1372nm (0.9eV). At room temperature energy of PL peak is shifted to ~1458nm (0.85eV). Origin of this emission is unclear. The peak has strong temperature dependence: the intensity decreases more than 20 times when the  $T_{\text{MEAS}}$  changes from 5 to 35 K.

## Electrical signatures:

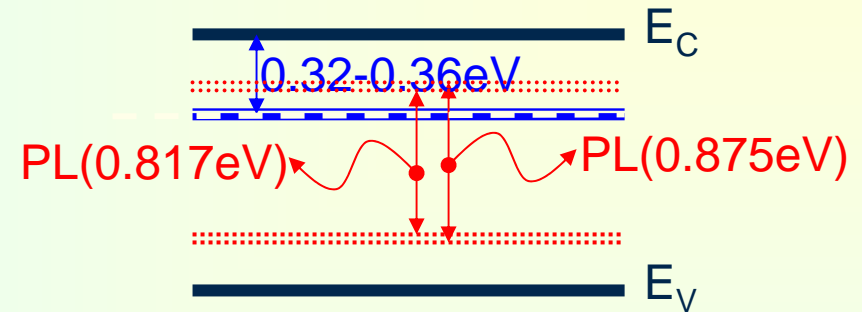
**DLTS:** Energy band is positioned at ~0.48eV from the conduction band.

*Possibly* PD has also **deep extended localized states**. This states may be related to irregular parts of PDs.

# Summary

## Dislocation dipoles:

- Appear after dissociation of plane defects
- Extended localized (mostly) and band-like states



## Optical signatures:

**PL:** PL peaks positioned at 1426nm ( $D_2$ , 0.875eV) and 1515nm ( $D_1$ , 0.817eV). Origins of this emissions are unclear.

## Electrical signatures:

**DLTS:** The energy level (levels) for these defects are positioned at 0.32 – 0.36 eV below the conduction band.